# Validation of the AnyBody full body musculoskeletal model in computing lumbar spine loads at L4L5 level

Tito Bassani [a,*], Elena Stucovitz [a], Zhihui Qian [b], Matteo Briguglio [a], Fabio Galbusera [a]

[a] IRCCS Istituto Ortopedico Galeazzi, Milan, Italy
[b] Key Laboratory of Bionic Engineering, Jilin University, Changchun, PR China

ABSTRACT

In the panorama of available musculoskeletal modeling software, AnyBody software is a commercial tool that provides a full body musculoskeletal model which is increasingly exploited by numerous researchers worldwide. In this regard, model validation becomes essential to guarantee the suitability of the model in representing the simulated system. When focusing on lumbar spine, the previous works aimed at validating the AnyBody model in computing the intervertebral loads held several limitations, and a comprehensive validation is to be considered as lacking.

The present study was aimed at extensively validating the suitability of the AnyBody model in computing lumbar spine loads at L4L5 level. The intersegmental loads were calculated during twelve specific exercise tasks designed to accurately replicate the conditions during which Wilke et al. (2001) measured in vivo the L4L5 intradiscal pressure. Motion capture data of one volunteer subject were acquired during the execution of the tasks and then imported into AnyBody to set model kinematics. Two different approaches in computing intradiscal pressure from the intersegmental load were evaluated. Lumbopelvic rhythm was compared with reference in vivo measurements to assess the accuracy of the lumbopelvic kinematics.

Positive agreement was confirmed between the calculated pressures and the in vivo measurements, thus demonstrating the suitability of the AnyBody model. Specific caution needs to be taken only when considering postures characterized by large lateral displacements. Minor discrepancy was found assessing lumbopelvic rhythm. The present findings promote the AnyBody model as an appropriate tool to noninvasively evaluate the lumbar loads at L4L5 in physiological activities.

© 2017 Elsevier Ltd. All rights reserved.

## 1. Introduction

Musculoskeletal models are advantageously exploited to non-invasively investigate the relation between human motion and internal biomechanical loads. When focusing on the characterization of human spine, musculoskeletal modeling can be accounted to evaluate the lumbar loads during physiological activities (e.g. training, ergonomics and rehabilitation) (El-Rich et al., 2004; Han et al., 2012; Raabe and Chaudhari, 2016; Grujicic et al., 2010; Stambolian et al., 2016; Tae Soo and Museong, 2010; Drake et al., 2006) and pathological scenarios (e.g. spine deformities and surgical fixation strategies) (Jalalian et al., 2013; Aubin et al., 2003; Curtin and Lowery, 2014; Hajizadeh et al., 2013; Bresnahan et al., 2010).

In the panorama of available modeling software, AnyBody software (AnyBody Technology, Denmark) is a commercial tool that provides a full body musculoskeletal model (AnyBody Managed Model Repository, AMMR). This model was developed by AnyBody Technology through collaboration in research projects with academic institutions (e.g. the lumbar spine model was developed by Hansen et al., 2006 and by de Zee et al., 2007) and is increasingly exploited by numerous researchers worldwide. Indeed, more than 50 publication references are listed in the AnyBody Technology web site for the year 2016, most of which exploit the full body model from AMMR. In this regard, model validation becomes essential to guarantee the suitability of the model in representing the simulated system (Hicks et al., 2015; Lund et al., 2012). To assess the validity of their lumbar model de Zee et al. (2007) compared the load calculated at L4L5 level during one specific posture with the corresponding value measured in vivo by Wilke et al. (2001). In that reference work Wilke et al. (2001) provided indeed an extended data set of the L4L5 intradiscal pressure, measured

during the execution of different postures, movements and loading conditions. In a more recent conference contribution, the reference values from Wilke et al. (2001) were used by Rasmussen et al. (2009) attempting to evaluate the suitability of the AnyBody full body model in computing the L4L5 load. Although in their study the authors pointed out a correspondence between computed loads and *in vivo* measurements, their work held several limitations. Only static postures were assessed, neglecting for motion conditions, and model kinematics was arbitrarily imposed to simulate the corresponding comparison tasks during which Wilke et al. (2001) measured the *in vivo* values. In addition, the dependence of the disc pressure on the flexion-extension, lateral bending and axial rotation motions provided by Wilke et al. (2001) was not compared. A further study by Rajaee et al. (2015) reported the agreement between the lumbar loads predicted by the AnyBody model and the *in vivo* values from Wilke et al. (2001) but only static lifting activities were evaluated and model kinematics was arbitrarily imposed to simulate the assessed conditions. Therefore, a comprehensive validation is to be considered as lacking.

The present study aims at extensively validating the ability of the AnyBody full body model in predicting lumbar loads at L4L5 level. Motion capture data of one volunteer subject were acquired during the execution of twelve specific tasks designed to accurately replicate different postures, movements and loading conditions assessed by Wilke et al. (2001). Motion data were imported into AnyBody to set model kinematics and the intersegmental loads at L4L5 level were computed during each task. The computed loads were processed according to two different approaches to obtain the corresponding intradiscal pressures, which were compared with the *in vivo* measurements. In addition, the lumbopelvic rhythm (i.e. the ratio of total lumbar rotation over pelvic rotation during trunk sagittal movement) was assessed during the trunk rotation tasks and the results were compared with reference *in vivo* measurements in order to evaluate the accuracy of the lumbopelvic kinematics.

## 2. Methods

### 2.1. Acquisition of the kinematic data

One male subject (28 years old) in good physical condition was enrolled to accurately replicate twelve exercise tasks during which Wilke et al. (2001) evaluated *in vivo* the L4L5 intradiscal pressure. The performed tasks are presented in Table 1. Weight and height of the volunteer matched those of the 45 years old subject (72 kg, 174 cm) assessed by Wilke et al. (2001). Since recognized that during lifting tasks the spinal loads are sensitive to the lifted load location, during the acquisitions the body postures and the lifted load locations were checked to replicate those depicted by Wilke et al. (2001 – Fig. 3). During the execution of the tasks the motion of the body segments was acquired at 70 Hz with an 8 cameras opto-

electronic BTS motion capture system (Smart-D, BTS Bioengineering, Garbagnate Milanese, Italy) in the Motion Analysis Laboratory at IRCCS Istituto Ortopedico Galeazzi. According to VICON Plug-in-Gait marker placement, 41 passive markers were placed on the skin in specific sites (Fig. 1). The markers trajectories in the 3D space were exported as *.c3d files and then loaded into AnyBody software to set mannequin kinematics (Fig. 2).

### 2.2. Musculoskeletal modeling

AnyBody software v.6 with full body musculoskeletal model (AMMR, v.1.6.3) was used for the analyses. The markers trajectories were low pass filtered with cut-off frequency of 10 Hz. Weight, height and anthropometric data of the evaluated subject were accounted to properly scale mass and length of the body segments. To characterize the external loads lifted during tasks vi, vii, viii and ix (Table 1), a 10 kg gravity oriented load was set at the centre of each hand. Differently, a 20 kg load was set at the solely right hand to describe the load carried during task xi. Evaluating the sitting task (xii), placement and dimensions of the sitting surface were set to match those of the stool used during the acquisition protocol. The AnyBody Motion Capture model was used to achieve motion and parameters optimization by best fitting the model with the recorded markers data. The distribution of the rotation angles in the lumbar joints, characterizing the so-called lumbar spine rhythm, was based on the continuous dynamic motion measurements of Wong et al. (2006). Muscle activations and internal reactions were computed through inverse dynamic analysis by minimizing muscles recruitment activation (Rasmussen et al., 2001; Damsgaard et al., 2006). The intersegmental reaction force acting in the L4L5 joint was evaluated during each task.

### 2.3. Comparison with the in vivo measurements

The axial component of the reaction force acting in the L4L5 joint (representing the axial compression from L4 to L5), was divided by the L4L5 disc area thus obtaining the average L4L5 disc pressure. The disc area (18 cm$^2$) was taken from Wilke et al. (2001) since obtained from the MRI evaluation of a subject having the same weight and height of the volunteer evaluated in the present study. However, it is known from *in vitro* studies (Brinckmann and Grootenboer, 1991; Nachemson, 1960) that the average disc pressure results lower than the disc nucleus pressure, which is that measured *in vivo* by Wilke et al. (2001). Thus, in order to properly compare the computed pressures with those obtained *in vivo*, the average disc pressure was corrected to obtain the nucleus pressure according to two different approaches. The first approach consisted in correcting the average pressure by the constant correction factor (i.e. 1.54) obtained from the *in vitro* tests (Brinckmann and Grootenboer, 1991; Nachemson, 1960). Differently, the second approach consisted in processing the average pressure and the flexion-extension rotation angle between L4 and L5 in the quadratic equation obtained from *in silico* study by Ghezelbash et al. (2016). The disc pressures obtained with correction factor (CF) and quadratic equation (QE) approaches were compared with the *in vivo* values from Wilke et al. (2001).

During tasks i, v, vi, vii, viii, ix and x the subject was asked to keep the position under assessment for three seconds and the average pressure was taken into account for the comparison. When assessing the flexion-extension task (ii), lateral bending (iii) and axial rotation (iv), Wilke et al. (2001) provided the intradiscal pressure in a dynamic continuous fashion, in dependence on the angle between the thoracolumbar junction (T12) and the sacrum. Accordingly, the same kind of analysis was performed in the present work. The subject was instructed to move slowly at his own pace. The angles between the thoracolumbar junction and the sacrum were obtained by processing the coordinates of the markers placed on thorax and pelvis. In order to compare one single pressure value for each task, the

**Table 1**
The twelve exercise tasks performed to replicate those evaluated by Wilke et al. (2001) and corresponding postures of the AnyBody full body mannequin. The short and the long red arrows depict respectively the 10 kg loads applied to each hand (which result overlaid in the lateral view) and the 20 kg load applied to the right hand during xi.

| i | ii | iii | iv | v | vi | vii | viii | ix | x | xi | xii |
|---|---|---|---|---|---|---|---|---|---|---|---|
| standing | flexion-extension | lateral bending | axial rotation | fingers to floor | lifting load[a] knees extended | arms at chest holding load[a] | arms extended holding load[a,c] | squat lifting load[a] | walking (compared to Wilke et al., 1999) | walking carrying load[b] | sitting (on stool, straight back) |



[a] Lifting with both hands a barbell loaded at the center with 20 kg, in order to replicate the lifting of a crate of beer of 19.8 kg of weight used in Wilke et al. (2001).
[b] Carrying with the right hand a dumbbell loaded with 20 kg.
[c] Barbell was held 60 cm away from chest, according to Wilke et al. (2001 – Fig. 3e).
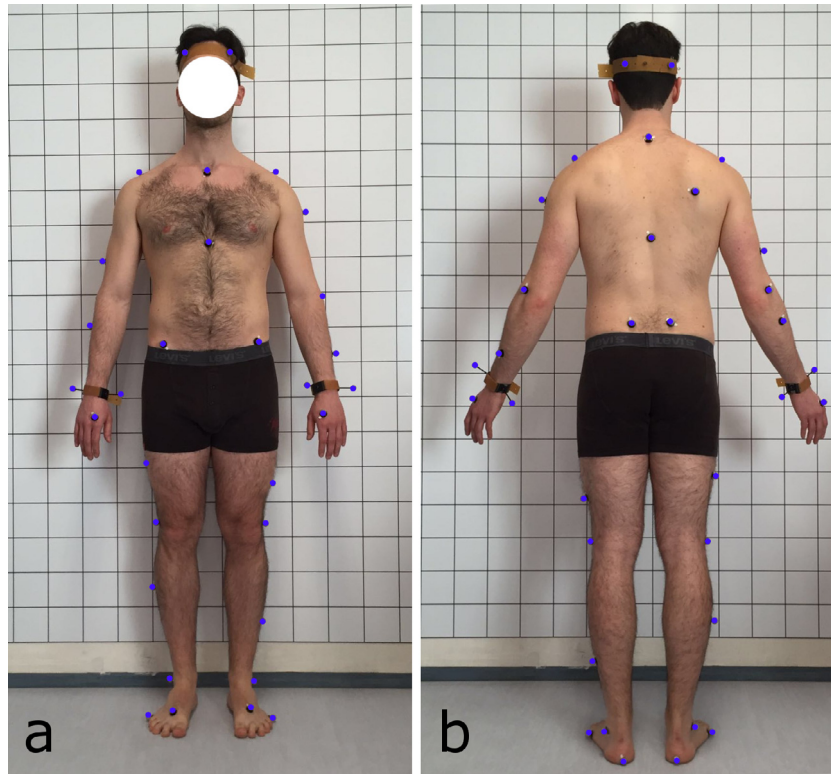
**Fig. 1.** Front (a) and back (b) view of the acquired subject with the 41 passive markers placed on the skin.
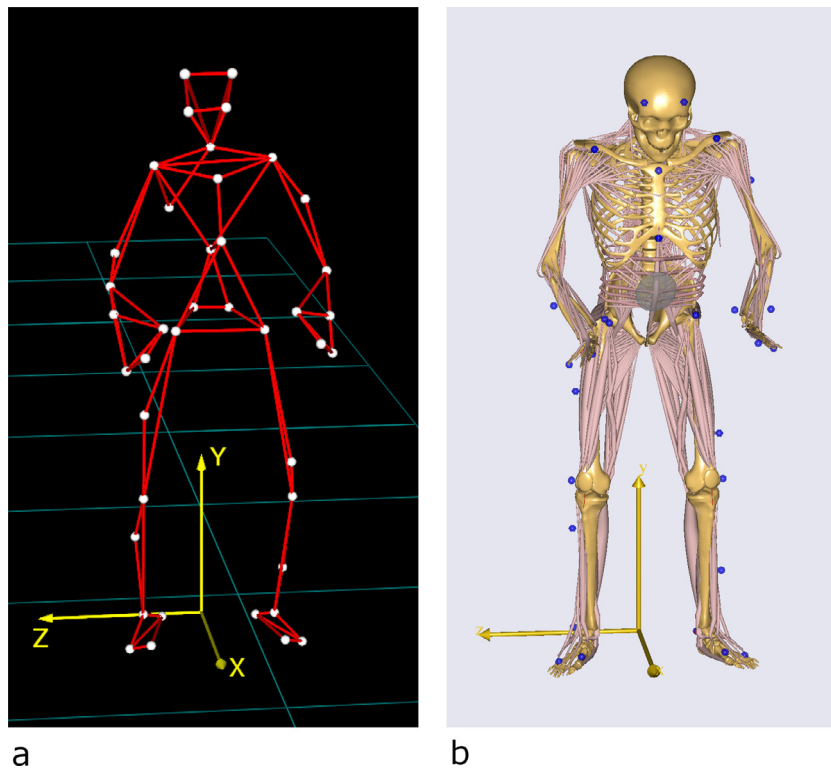


**Fig. 2.** The markers positions in the 3D space acquired with BTS motion capture software (a) and subsequently imported to set the AnyBody mannequin kinematic (b).

corresponding values in ii, iii and iv were obtained by averaging the pressure found at ±20° considering tasks ii and iv, and at ±15° considering task iii. The *in vivo* corresponding values were visually inferred from Wilke et al. (2001 – Fig. 2). During the walking tasks (x and xi) the average pressure measured during the walking cycle was chosen for the comparison. The calculated pressures were checked to be normally distributed and the agreement with the *in vivo* measurements was then assessed using Pearson correlation coefficient, ranging from −1 to 1. The statistical significance of the coefficient was tested according to two-tailed *t*-test at 0.05 significance level.

### 2.4. Assessment of the lumbopelvic rhythm

The lumbopelvic rhythm calculated during the trunk flexion and extension movements was compared with the reference values reported by Tafazzol et al. (2014). The extension condition was evaluated from the flexion-extension task (ii), whereas the flexion condition was assessed from the finger to floor task (v). This choice was motivated by the need of assessing comparable maximum trunk flexion angles. Indeed, while during ii the subject flexed forward up to 40°, during v the movement started from upright standing (0°) and reached 115° thus allowing for the comparison with the reference flexion value (121°, Table 2) provided by Tafazzol et al. (2014). According to Tafazzol et al. (2014) the following changes in orientation with respect to the upright standing posture were considered: changes in orientation of the sacrum with respect to the global coordinate system (P); changes in orientation of the thorax with respect to the global coordinate system (T); changes in relative orientation of L1 and sacrum (L). The lumbopelvic ratio (L/P) was subsequently calculated for 10 intervals of trunk flexion and extension in the sagittal plane (Tafazzol et al., 2014).

## 3. Results

The assessment of disc pressure in dependence on the angle between the thoracolumbar junction and the sacrum pointed out values comparable with the *in vivo* measurements during flexion-extension (Fig. 3a and b) and axial rotation (Fig. 3e and f), whereas differences were found in lateral bending when the angle exceeded ±15° (Fig. 3c and d). In detail, the pressure values calculated with the CF approach resulted from 0.1 to 0.2 MPa higher than those computed with the QE approach (Fig. 3a, c, and e). In flexion-extension at ±20° the values calculated with CF, QE, and the *in vivo* measurements resulted around 0.7, 0.6 and 0.7 MPa, respectively (Fig. 3a and b), and in axial rotation at ±20° they were found around 0.5, 0.3 and 0.6 MPa (Fig. 3e and f). During lateral bending the pressures resulted between 0.3 and 0.6 MPa for rotation angles lower than ±15° (Fig. 3c and d) but differently from the *in vivo* measurement the calculated CF and QE pressures increased rapidly to 1.5 and 1.2 MPa when approaching ±20° instead remaining below 0.6 MPa (Fig. 3c and d). In fingers to floor task (v) the calculated pressures resulted lower than that found *in vivo*, i.e. 1 and 0.9 MPa with CF and QE vs 1.6 MPa found *in vivo* (Fig. 4). For the other conditions, the following results were pointed out (Fig. 4): 0.4, 0.3 and 0.5 MPa in standing (i); 2.3, 1.9 and 2.3 MPa in lifting load, knees extended (vi); 0.9, 0.7 and 1 MPa in arms at chest lifting

load (vii); 1.7, 1.4 and 1.8 MPa in arms extended lifting load (viii); 1.9, 1.7 and 1.7 MPa in squat lifting load (ix); 0.5, 0.4 and 0.6 MPa in walking (x); 1.3, 1 and 1 MPa in walking carrying load (xi); 0.4, 0.3 and 0.5 MPa in sitting (xii). Significant very strong correlations were found between the *in vivo* measurements and the pressures values calculated according to both CF and QE approaches (Fig. 5). The regression analysis, which assesses the linear relation between the compared pressures, showed similar line slope, intercept and root mean squared error (RMSE) for both CF and QE (Fig. 5).

The lumbopelvic ratio (L/P) was found ranging from 0.45 to 1.92 in the 10 intervals of trunk flexion, and from 0.04 to 0.71 during trunk extension (Table 2). In both cases, the progression of L/P from standing (0–10%) to full bending (90–100%) exhibited random-shaped variations without progressively increasing or decreasing as in Tafazzol et al. (2014) (Table 2).

## 4. Discussion

The results revealed that the AnyBody model is suitable in describing the dependence between disc pressure and motion angles during flexion-extension and axial rotation (Fig. 3a, b and e, f). In lateral bending the model provided adequate values only for motion angles lower than ±15° (Fig. 3c). The steep increase of disc pressure when the angle exceeded ±15° can be related to over-activations of the recruited muscles and suggests to account for that postural limit when setting movement parameters in AnyBody model. The pressure values calculated with the CF approach resulted from 0.1 to 0.2 MPa higher than those computed with the QE approach (Fig. 3). This difference in the results was confirmed in all the evaluated tasks (Fig. 4). In this regard, while CF is based on constant correction factor from *in vitro* tests, QE was derived from *in silico* study by Ghezelbash et al. (2016) with the aim of accounting for the effect of the relative flexion-extension angle between L4 and L5 (evaluated from −2° to 11°, positive in flexion) on disc pressure. Specifically, Ghezelbash et al. (2016) reported increasing disc pressure in dependence on increasing rotation angle at given axial compression. Moreover, the pressure increasing was found maximum in case of absence of axial compression and proportionally decreased in function of higher compression conditions. In the present work the axial compression was never negligible (due to the presence of the upper body weight) and the rotation angle between L4 and L5 was found moderate in the considered tasks (ranging from −1.7° to +5.9°) thus justifying the lower pressure values found with QE approach.

However, despite this constant and moderate difference found between CF and QE, the agreement between the calculated

**Table 2**
Lumbopelvic angles and lumbopelvic ratios computed with AnyBody model during trunk flexion and extension, in comparison with the corresponding values from Tafazzol et al. (2014).

| Full range of thorax (T), pelvic (P), lumbar spine (L), and T to L1 rotations during forward flexion to reach full flexion angle | | | | | |
|---|---|---|---|---|---|
| | Thorax flexion T [°] | Pelvic flexion P [°] | Lumbar flexion L [°] | T5-L1 relative motion [°] | Time to full flexion [s] |
| AnyBody | 115 | 56.6 | 43.7 | 15.0 | 2.4 |
| Tafazzol et al. (2014) | 121 | 53.0 | 60.2 | 8.3 | 5.2 |

| Lumbopelvic ratios (L/P) for 10 intervals of trunk flexion (i.e., 0–10%, 10–20%, ..., and 90–100% of full trunk flexion) | | | | | | | | | | |
|---|---|---|---|---|---|---|---|---|---|---|
| | 0–10% | 10–20% | 20–30% | 30–40% | 40–50% | 50–60% | 60–70% | 70–80% | 80–90% | 90–100% |
| AnyBody | 1.31 | 0.93 | 1.47 | 0.85 | 0.49 | 1.17 | 1.85 | 1.92 | 1.34 | 0.45 |
| Tafazzol et al. (2014) | 2.57 | 2.52 | 2.35 | 2.24 | 2.11 | 1.97 | 1.82 | 1.60 | 1.35 | 1.14 |

| Lumbopelvic ratios (L/P) for 10 intervals of trunk extension (i.e., 0–10%, 10–20%, ..., and 90–100% of full trunk extension) | | | | | | | | | | |
|---|---|---|---|---|---|---|---|---|---|---|
| | 0–10% | 10–20% | 20–30% | 30–40% | 40–50% | 50–60% | 60–70% | 70–80% | 80–90% | 90–100% |
| AnyBody | 0.71 | 0.34 | 0.50 | 0.66 | 0.24 | 0.04 | 0.37 | 0.36 | 0.11 | 0.27 |
| Tafazzol et al. (2014) | 1.07 | 1.31 | 1.57 | 1.79 | 1.98 | 2.14 | 2.31 | 2.51 | 2.71 | 2.90 |
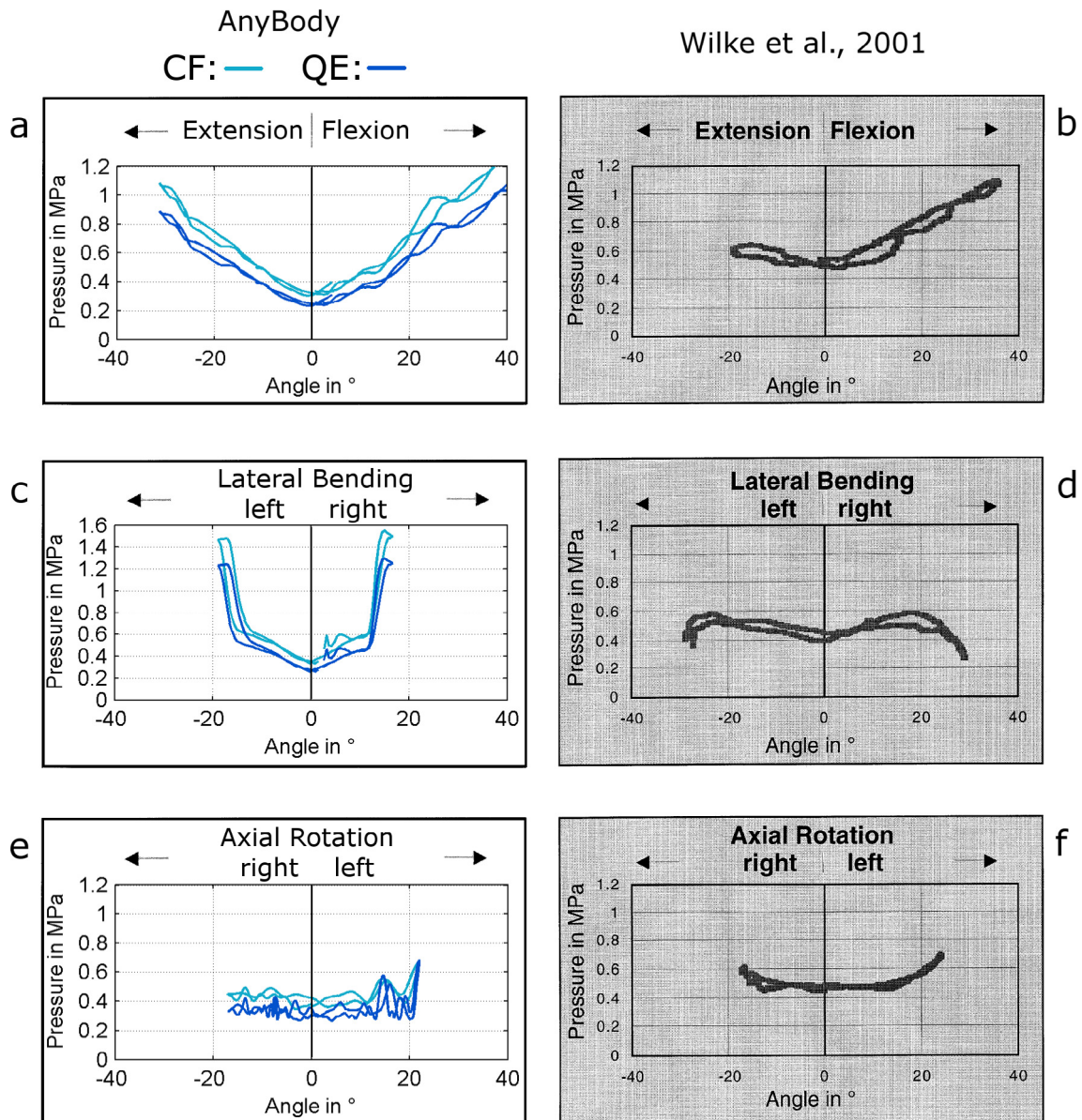
**Fig. 3.** L4L5 disc pressure in dependence on the angle between the thoracolumbar junction and the sacrum (with respect to the total motion), calculated with AnyBody model (left column) according to CF and QE approaches (depicted in light blue and dark blue, respectively) and measured *in vivo* by Wilke et al. (2001) (right column) during flexion-extension (a, b), lateral bending (c, d) and axial rotation tasks (e, f). The reference plots in the right column are reprinted from the original paper (Wilke et al., 2001– Fig. 2) with courteous publisher permission. (For interpretation of the references to color in this figure legend, the reader is referred to the web version of this article.)

pressures and the *in vivo* measurements was generally confirmed during all tasks, with the sole exception of fingers to floor condition (Fig. 4). The lower pressure found during fingers to floor (1 and 0.9 MPa with CF and QE, respectively) in comparison with 1.6 MPa found *in vivo* can be related to neglecting the role of the intervertebral anteroposterior shear when computing disc pressure. Indeed, in the present study the sole intersegmental compression force was accounted to calculate disc pressure whereas during fingers to floor posture a significant contribution from the antero-posterior shear is expected. Otherwise, a different simpler explanation can be proposed. Indeed, the pressure value reported by Wilke et al. (2001) during fingers to floor (1.6 MPa) was interpreted in the present study as characterizing the subject posture with fingertips touching floor (as shown with concise specifications in the photograph in Wilke et al., 2001 – Fig. 3c). But it is not to exclude that the reported value had been obtained as the maximum pressure value found inside the whole finger to floor exercise, from upright

standing to reaching floor. Under this assumption, the maximum pressure found with AnyBody during the whole exercise was 1.4 and 1.2 MPa (obtained with CF and QE, respectively, in correspondence of 95° of trunk flexion before fingertips reached floor) which results more similar to 1.6 MPa reported by Wilke et al. (2001).

Concerning the strength of the relation between the calculated values and the *in vivo* measurements, very strong significant correlation was confirmed using both the CF and QE approaches (Fig. 5). In particular, the regression analysis revealed that the incremental agreement, which is the optimum when the slope of the regression line corresponds to the bisector, was found preferable for CF (line slope equal to 43°, Fig. 5) with respect to that of QE (39°). This finding is related to the tendency of QE to provide pressure values lower than those obtained with CF (Figs. 3 and 4). The offset effects were negligible (see intercept values, Fig. 5) and both CF and QE performed equally in terms of goodness of fit (see root mean square error, RMSE, in Fig. 5).
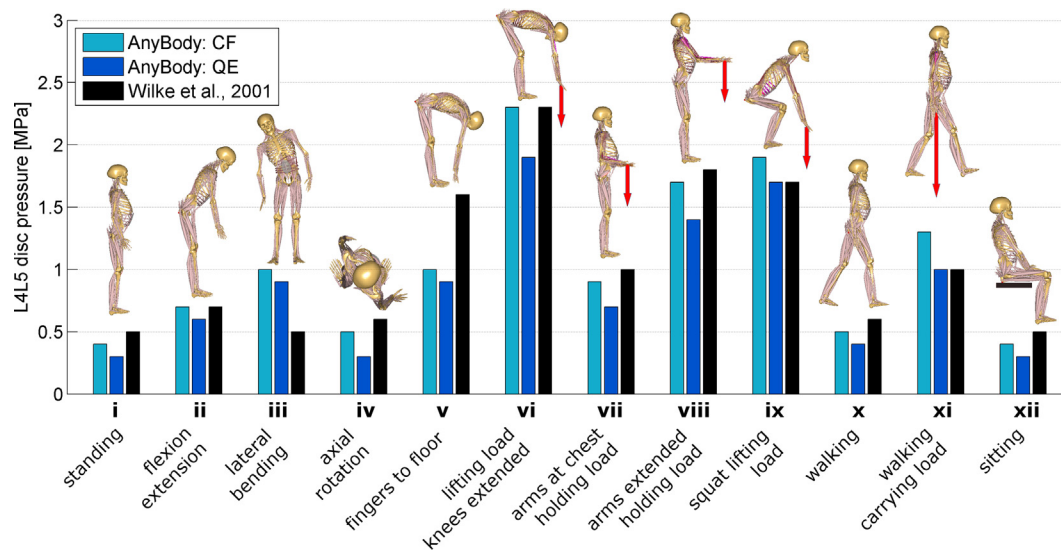
**Fig. 4.** L4L5 disc pressure calculated with AnyBody model according to CF and QE approaches (presented in light blue and dark blue, respectively) and measured *in vivo* by Wilke et al. (2001) (presented in black) in the specific task. The red arrows depict the 10 kg load applied to each hand during straight legs lifting load, arms at chest holding load, arms extended holding load and squat lifting load tasks, and the 20 kg load applied to the solely right hand during walking carrying load task. (For interpretation of the references to color in this figure legend, the reader is referred to the web version of this article.)
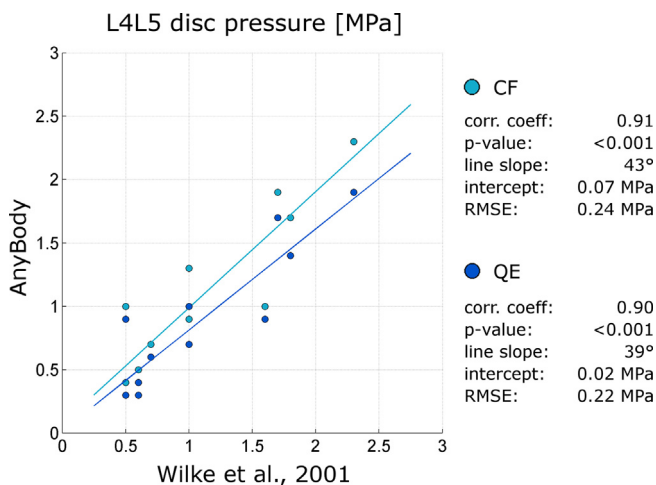


**Fig. 5.** Scatter plots of the L4L5 disc pressure calculated with AnyBody model (vertical axis) according to CF and QE approaches (depicted in light blue and dark blue, respectively) and of those measured *in vivo* by Wilke et al. (2001) (horizontal axis) during the evaluated tasks. Pearson correlation coefficient along with its significance, and regression line slope, intercept and root mean square error (RMSE) are presented in the right panel. (For interpretation of the references to color in this figure legend, the reader is referred to the web version of this article.)

Regarding the evaluation of the lumbosacral kinematics, the progression of the lumbopelvic ratio (L/P, Table 2) during trunk flexion and extension did not confirm the previous values from Tafazzol et al. (2014). Indeed, Tafazzol et al. (2014) pointed out that with respect to pelvis the lumbar spine contributed more to the trunk rotation during early and final stages of flexion and extension, respectively (L/P progressively decreases or increases in the two cases). Conversely, random-shaped variations of L/P were found in the present work. These results can be principally related to the lower lumbar flexibility (see L, in Table 2) and concomitant higher thoracolumbar mobility (see T5-L1) of the evaluated subject in comparison with the reference values. Further developments are thus necessary to better investigate this lack of agreement by extending the evaluation to additional subjects with different characteristics of spine flexibility. Nonetheless, it is worth considering

that although the overall lumbar spine motion was computed by processing the markers position of T10 and superior iliac spine (Fig. 1), the lumbopelvic ratio was obtained by accounting for the orientations of L1 and sacrum as calculated with the model (see Methods section). To this regard, the orientation of L1 depends on the definition of the lumbar spine rhythm assumption, which determinates how the motion is distributed at the different lumbar levels. In the present model from the AnyBody repository the lumbar spine rhythm was based by default on Wong et al. (2006). This setting is known to provide, from lower to upper levels, the increasing relative contribution of the individual vertebral segments to the overall lumbar motion (Han et al., 2012). This result can be observed in the present study when evaluating the rotations of the lumbar segments during the flexion-extension, lateral bending and axial rotation tasks (Fig. 6). It is worth noting that the obtained rotations are in agreement with the reference *in vivo* measurements from Aiyangar et al. (2014) and Gercek et al. (2008). Nevertheless, basing the lumbar spine rhythm on literature values can represent a potential limitation since it could not interpret in principle the real vertebral motion pattern of the evaluated subject. To this regard, Arshad et al. (2016) demonstrated e.g. that different lumbar spine rhythms can affect the distribution of the lumbar spine loads. Accordingly, future developments are necessary to clarify whether further spine rhythm assumptions can provide differences in the prediction of the L1 orientation and thus in the calculation of the lumbopelvic ratio.

The present study has several limitations: one subject and one repetition of the tasks were evaluated, and comparison only with Wilke et al. (2001) was performed (indeed, the tasks were designed to closely match those described in Wilke et al., 2001). Subject was 28 years old whereas the one enrolled by Wilke et al. (2001) was 45 years old. The AnyBody model has several limitations (i.e. rigid rib cage and thoracic spine, no facet joints and ligaments, lumbar discs simply described as spherical joints) and might be improved. Nevertheless, the validity of these modeling assumptions is supported by other studies (Ignasiak et al., 2016; Ghezelbash et al., 2015; Meng et al., 2015). However, the aim of the present study was to validate the ability of the AnyBody model to predict the lumbar load at L4L5, specifically for the model available in the repository which is used by several researchers worldwide, and not for improved versions which would be not so widely available.
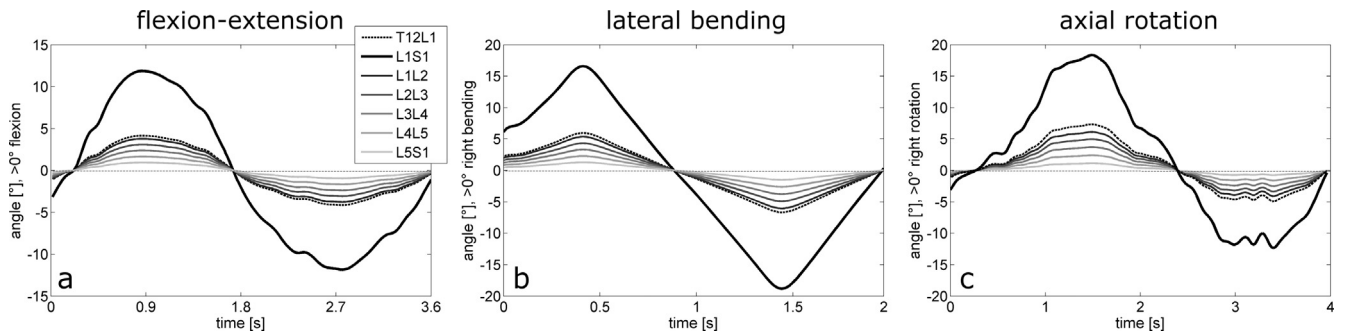
**Fig. 6.** Intersegmental relative rotation angles of thoracolumbar and lumbosacral levels calculated with the AnyBody model during flexion-extension (a), lateral bending (b) and axial rotation (c) tasks. The angle at thoracolumbar level (T12L1) is presented as dashed black line. The angle between L1 and the sacrum (L1S1, the whole lumbar section) is depicted as bold solid black line. The angles of the lumbar segments (L1L2, L2L3, L3L4, L4L5, L5S1), the sum of which gives the L1S1 angle, are depicted as solid lines in grey scale (from dark to light hue proceeding from L1L2 to L5S1 level).

In conclusion, the results of the present work demonstrate the suitability of the AnyBody full body musculoskeletal model in computing lumbar spine load at L4L5 level. Specific caution needs to be taken only when considering postures characterized by large lateral displacements. Nevertheless, the present findings promote the AnyBody model as an appropriate tool to non-invasively evaluate lumbar loads and infer intervertebral disc pressure in physiological activities. Further developments extending the present analyses to other comparable subjects are required to better clarify the minor discrepancy pointed out in the assessment of the lumbopelvic rhythm. Future studies will evaluate the use of AnyBody modeling to describe intervertebral loads in pathological conditions known altering spine alignment (e.g. spine deformities and vertebral fixation surgeries), by accounting for example for the *in vivo* measurements reported by Meir et al. (2007) in scoliosis and by Rohlmann et al. (1995) in the assessment of spine fixation.

### Conflict of interest statement

The authors certify that there is no conflict of interest with any organization regarding the material discussed in the manuscript.

### Acknowledgments

### Appendix A. Supplementary material

Supplementary data associated with this article can be found, in the online version, at http://dx.doi.org/10.1016/j.jbiomech.2017.04.025.

### References

Aiyangar, A.K., Zheng, L., Tashman, S., Anderst, W.J., Zhang, X., 2014. Capturing three-dimensional in vivo lumbar intervertebral joint kinematics using dynamic stereo-X-ray imaging. J. Biomech. Eng. 136 (1), 011004.

Arshad, R., Zander, T., Dreischarf, M., Schmidt, H., 2016. Influence of lumbar spine rhythms and intra-abdominal pressure on spinal loads and trunk muscle forces during upper body inclination. Med. Eng. Phys. 38 (4), 333–338.

Aubin, C.E., Petit, Y., Stokes, I.A., Poulin, F., Gardner-Morse, M., Labelle, H., 2003. Biomechanical modeling of posterior instrumentation of the scoliotic spine. Comput. Methods Biomech. Biomed. Eng. 6, 27–32.

Bresnahan, L., Fessler, R., Natarajan, R.N., 2010. Evaluation of change in muscle activity as a result of posterior lumbar spine surgery using a dynamic modeling system. Spine 35 (16), E761–E767.

Brinckmann, P., Grootenboer, H., 1991. Change of disc height, radial disc bulge, and intradiscal pressure from discectomy: an in vitro investigation on human lumbar discs. Spine (Phila Pa 1976) 16 (6), 641–646.

Curtin, M., Lowery, M., 2014. Musculoskeletal modelling of muscle activation and applied external forces for the correction of scoliosis. J. Neuroeng. Rehabil. 11, 52.

Damsgaard, M., Rasmussen, J., Christensen, S.T., Surma, E., de Zee, M., 2006. Analysis of musculoskeletal systems in the AnyBody modeling system. Simul. Model. Pract. Theory 14, 1100–1111.

de Zee, M., Hansen, L., Wong, C., Rasmussen, J., Simonsen, E.B., 2007. A generic detailed rigid-body lumbar spine model. J. Biomech. 40, 1219–1227.

Drake, J.D.M., Fischer, S.L., Brown, S.H.M., Callaghan, J.P., 2006. Do exercise balls provide a training advantage for trunk extensor exercises? A biomechanical evaluation. J. Manipulative. Physiol. Ther. 29 (5), 354–362.

El-Rich, M., Shirazi-Adl, A., Arjmand, N., 2004. Muscle activity, internal loads, and stability of the human spine in standing postures: combined model and in vivo studies. Spine (Phila Pa 1976) 29 (23), 2633–2642.

Gercek, E., Hartmann, F., Kuhn, S., Degreif, J., Rommens, P.M., Rudig, L., 2008. Dynamic angular three-dimensional measurement of multisegmental thoracolumbar motion in vivo. Spine (Phila Pa 1976) 33 (21), 2326–2333.

Ghezelbash, F., Arjmand, N., Shirazi-Adl, A., 2015. Effect of intervertebral translational flexibilities on estimations of trunk muscle forces, kinematics, loads, and stability. Comput. Methods Biomech. Biomed. Eng. 18 (16), 1760–1767.

Ghezelbash, F., Shirazi-Adl, A., Arjmand, N., El-Ouaaid, Z., Plamondon, A., 2016. Subject-specific biomechanics of trunk: musculoskeletal scaling, internal loads and intradiscal pressure estimation. Biomech. Model. Mechanobiol. 15 (6), 1699–1712.

Grujicic, M., Pandurangan, B., Xie, X., Gramopadhye, A., Wagner, D., Ozen, M., 2010. Musculoskeletal computational analysis of the influence of car-seat design/adjustments on long-distance driving fatigue. Int. J. Ind. Ergonom. 40 (3), 345–355.

Hajizadeh, K., Huang, M., Gibson, I., Gabriel, Liu., 2013. Developing a 3d multi-body model of a scoliotic spine during lateral bending for comparison of ribcage flexibility and lumbar joint loading to the normal model. In: ASME International Mechanical Engineering Congress and Exposition (IMECE2013).

Han, K.S., Zander, T., Taylor, W.R., Rohlmann, A., 2012. An enhanced and validated generic thoraco-lumbar spine model for prediction of muscle forces. Med. Eng. Phys. 34, 709–716.

Hansen, L., de Zee, M., Rasmussen, J., Andersen, T.B., Wong, C., Simonsen, E.B., 2006. Anatomy and biomechanics of the back muscles in the lumbar spine with reference to biomechanical modeling. Spine (Phila Pa 1976) 31 (17), 1888–1899.

Hicks, J.L., Uchida, T.K., Seth, A., Rajagopal, A., Delp, S.L., 2015. Is my model good enough? Best practices for verification and validation of musculoskeletal models and simulations of movement. J. Biomech. Eng. 137 (2), 020905.

Ignasiak, D., Ferguson, S.J., Arjmand, N., 2016. A rigid thorax assumption affects model loading predictions at the upper but not lower lumbar levels. J. Biomech. 49 (13), 3074–3078.

Jalalian, A., Gibson, I., Tay, E.H., 2013. Computational biomechanical modeling of scoliotic spine: challenges and opportunities. Spine Deform. 1 (6), 401–411.

Lund, M.E., de Zee, M., Andersen, M.S., Rasmussen, J., 2012. On validation of multibody musculoskeletal models. Proc. Inst. Mech. Eng. H 226 (2), 82–94.

Meir, A.R., Fairbank, J.C., Jones, D.A., McNally, D.S., Urban, J.P., 2007. High pressures and asymmetrical stresses in the scoliotic disc in the absence of muscle loading. Scoliosis 2, 4.

Meng, X., Bruno, A.G., Cheng, B., Wang, W., Bouxsein, M.L., Anderson, D.E., 2015. Incorporating six degree-of-freedom intervertebral joint stiffness in a lumbar spine musculoskeletal model-method and performance in flexed postures. J. Biomech. Eng. 137 (10), 101008.

Nachemson, A., 1960. Lumbar intradiscal pressure. Experimental studies on post-mortem material. Acta Orthop. Scand. Supplementum 43, 1–104.

Raabe, M.E., Chaudhari, A.M.W., 2016. An investigation of jogging biomechanics using the full-body lumbar spine model: model development and validation. J. Biomech. 49 (7), 1238–1243.

Rajaee, M.A., Arjmand, N., Shirazi-Adl, A., Plamondon, A., Schmidt, H., 2015. Comparative evaluation of six quantitative lifting tools to estimate spine loads during static activities. Appl. Ergon. 48, 22–32.

Rasmussen, J., Damsgaard, M., Voigt, M., 2001. Muscle recruitment by the min/max criterion—a comparative numerical study. J. Biomech. 34, 409–415.

Rasmussen, J., de Zee, M., Carbes, S., 2009. Validation of a biomechanical model of the lumbar spine. In: XXIInd Congress of the International Society of Biomechanics.

Rohlmann, A., Bergmann, G., Graichen, F., Mayer, H.M., 1995. Telemeterized load measurement using instrumented spinal internal fixators in a patient with degenerative instability. Spine (Phila Pa 1976) 15;20 (24), 2683–2689.

Stambolian, D., Eltoukhy, M., Asfour, S., 2016. Development and validation of a three dimensional dynamic biomechanical lifting model for lower back evaluation for careful box placement. Int. J. Ind. Ergon. 54, 10–18.

Tae Soo, B., Museong, M., 2010. Effect of lumbar lordotic angle on lumbosacral joint during isokinetic exercise: a simulation study. Clin. Biomech. (Bristol, Avon) 25 (7), 628–635.

Tafazzol, A., Arjmand, N., Shirazi-Adl, A., Parnianpour, M., 2014. Lumbopelvic rhythm during forward and backward sagittal trunk rotations: combined in vivo measurement with inertial tracking device and biomechanical modeling. Clin. Biomech. (Bristol, Avon) 29 (1), 7–13.

Wilke, H.J., Neef, P., Caimi, M., Hoogland, T., Claes, L.E., 1999. New in vivo measurements of pressures in the intervertebral disc in daily life. Spine (Phila Pa 1976) 24, 755–762.

Wilke, H.J., Neef, P., Hinz, B., Seidel, H., Claes, L., 2001. Intradiscal pressure together with anthropometric data – a data set for the validation of models. Clin. Biomech. (Bristol, Avon) 16 (Suppl 1), S111–S126.

Wong, K.W., Luk, K.D., Leong, J.C., Wong, S.F., Wong, K.K., 2006. Continuous dynamic spinal motion analysis. Spine (Phila Pa 1976) 31 (4), 414–419.